Wurtzite structure in ultrathin ZnO films on Fe(110): Surface x-ray diffraction and *ab initio* calculations

H. L. Meyerheim,[1,*] A. Ernst,[1,2,†] K. Mohseni,[1] C. Tusche,[1] W. A. Adeagbo,[3] I. V. Maznichenko,[3] W. Hergert,[3] G. R. Castro,[4] J. Rubio-Zuazo,[4] A. Morgante,[5] N. Jedrecy,[6] I. Mertig,[1,3] and J. Kirschner[1,3]

[1]*Max-Planck-Institut für Mikrostrukturphysik, Weinberg 2, D-06120 Halle, Germany*

[2]*Wilhelm-Ostwald-Institut für Physikalische und Theoretische Chemie, Universität Leipzig, Linnéstraße 2, 04103 Leipzig, Germany*

[3]*Institut für Physik, Martin-Luther-Universität Halle-Wittenberg, D-06099 Halle, Germany*

[4]*ESRF, Boîte Postale 220, F-38043 Grenoble Cedex, France*

[5]*TASC-INFM National Laboratory, I-34012 Basovizza, Italy*

[6]*Institut des Nano Sciences de Paris, UPMC-Sorbonne Universités, CNRS-UMR7588, 75005 Paris, France*

(Received 31 July 2013; revised manuscript received 30 July 2014; published 20 August 2014)

Using surface x-ray diffraction in combination with *ab initio* calculations we have studied the atomic structure of ultra-thin ZnO films deposited on Fe(110). In contrast to expectation that ZnO adopts the "graphitic" hexagonal Boron-nitride structure to the Wurtzite (WZ) structure is observed. Its formation is related to oxygen impurities in Fe(110) hollow sites inducing an anisotropic charge redistribution within the film which is characterized by a metallic surface. Our results provide a deeper understanding of depolarization mechanisms in ultrathin polar films at the atomic scale.

DOI: 10.1103/PhysRevB.90.085423 PACS number(s): 68.55.ag, 61.05.cp, 71.15.Mb, 81.05.Dz

Zinc oxide (ZnO) is an often employed semiconductor with wide prospects in optoelectronic, catalysis [1], and lasing applications [2]. Also, ZnO has attracted considerable interest in fundamental studies considering magnetism [3] and regarding the instability of polar {0001} surfaces. The latter case is due to the fact that the ZnO structure, characterized by alternating layers of zinc and oxygen atoms along the c axis, lacks inversion symmetry (space group $P6_3mc$). According to the classification of Tasker [4] ZnO{0001} corresponds to the type III ionic surfaces which are inherently unstable owing to the divergence of the electrostatic potential. Possible stabilization mechanisms have been discussed in the past based on theoretical and experimental studies involving complex structural rearrangements, charge transfer, and adsorption of foreign species [5–9].

On the other hand, nanosized polar crystals are much less investigated. Several experimental studies on ultrathin films have not identified the "classical" depolarization mechanisms which are at work for bulk crystals [10–15]. For instance, in the case of ZnO films, depolarization is achieved by the transition of the polar wurtzite (WZ) structure to the nonpolar "graphitic" hexagonal boron-nitride (h-BN) structure in which zinc and oxygen atoms are threefold coordinated in flat hexagonal sheets [13–15].

Theoretical studies have shown [16–18] that despite the absence of the actual divergence of the electrostatic potential in ultrathin films a certain critical thickness exists above which a polar instability sets in, involving the presence of compensating surface charges. In the case of ZnO this leads to a transformation from the h-BN to the WZ structure predicted to take place at nine monolayers (ML) film thickness [19] (here and in the following we refer to one ML for one Zn-O double layer).

On the other hand, experimental evidence of polar thin films with compensating surface charges is surprisingly scarce. The previous surface x-ray diffraction (SXRD) study of ZnO on Ag(111) has provided evidence for the h-BN to WZ transformation, albeit taking place at a lower film thickness than theoretically predicted (beginning above about four ML [13]). However, a clear-cut proof for the correlation between the h-BN to WZ phase transformation and the presence of a classical depolarization mechanism involving surface charges, defects, or metallization has not been provided.

In this paper we show by a combined SXRD and theoretical study that oxygen ("impurity") atoms located at the interface between an ultrathin ZnO film and the Fe(110) substrate crystal induce a decoupling of the ZnO film from the substrate and a redistribution of charge within the ZnO film characterized by a metallic surface. This stabilizes the WZ structure in the thickness range (<4 ML) where otherwise the h-BN structure is stable. Thereby, the depolarization of the WZ film is achieved by the metallisation of the surface layer. Our result is a direct proof of previous theoretical predictions [17,18] and provides a deeper understanding of the complex polarity compensation mechanisms in ultrathin polar films at the atomic scale.

The Fe(110) crystal was cleaned by standard methods [20] until only trace amounts of carbon and nitrogen were detected by Auger electron spectroscopy (AES). ZnO was deposited under an ambient oxygen pressure of $p_{O_2} = 1 \times 10^{-7}$ mbar by evaporation from a polycrystalline ZnO rod heated by electron bombardment. The sample was annealed up to 530 K to improve long range order. Annealing at higher temperatures resulted in a decomposition of the ZnO film by evaporation of Zn. Thickness calibration was carried out by AES and *ex posteriori* by SXRD and scanning tunneling microscopy (STM). We have studied samples with a nominal film thickness of 1.5 and 2.9 MLs, which exhibit three and four fractionally occupied ZnO (double) layers, respectively, as shown schematically in Fig. 1(a). The 2.9 ML film has two completely filled ZnO layers.

*hmeyerhm@mpi-halle.mpg.de
†aernst@mpi-halle.mpg.de

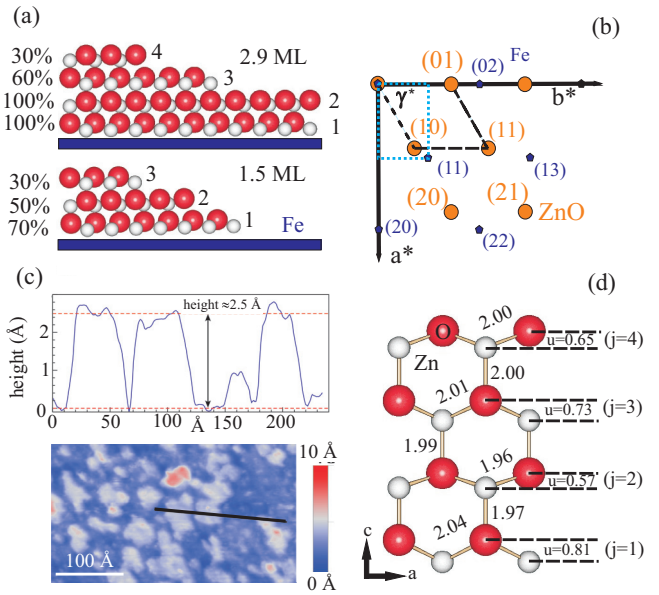

FIG. 1. (Color online) (a) Schematic view of the ZnO films (1.5 and 2.9 ML) showing the layer fillings (see also labels on the left). Large (red) and small (gray) balls represent oxygen and Zn atoms, respectively. (b) a^*-b^* plane of the reciprocal lattice of ZnO/Fe(110). Small (blue) and large (yellow) symbols represent Fe(110) and ZnO rods. The unit cells of the ZnO film and the Fe(110) surface are indicated by the dashed and dotted lines, respectively. (c) 440 × 250 Å^2 STM (constant current) image of ≈3 ML ZnO on Fe(110) (sample bias $U = +1.6$ eV, $I = 300$ pA) and a 240 Å profile showing an apparent step height of 2.5 Å. (d) Structure model for 2.9 ML ZnO/Fe(110). Distances are in Å units.

The SXRD experiments were carried out at the beamline BM25b of the European Synchrotron Radiation Facility (Grenoble, France) and at the ALOISA beamline of the Elettra Synchrotron (Trieste, Italy) using a six circle and a z-axis diffractometer, respectively. Samples were prepared *in situ* followed by collection of integrated reflection intensities [$I_{\rm obs}(hk\ell)$] along q_z, the momentum transfer normal to the sample surface in reciprocal space ($q_z = \ell \times c^*$, where $c^* = 1/c_0$) under grazing incidence of the incoming x-ray beam.

Figure 1(b) shows a schematic view of the reciprocal lattice projected along q_z which is parallel to the [110] axis of the Fe crystal [21]. Large circles and small pentagons correspond to the rods of the ZnO film and the Fe-substrate crystal truncation rods (CTRs), respectively. The in-plane reflection indices (hk) of ZnO (large) and Fe(110) (small) are labeled next to the symbols. The analysis of the positions of the first order film rods, $(10)_{\rm ZnO}$ and $(01)_{\rm ZnO}$, indicates that the ZnO film grows in an incommensurate relationship relative to the substrate: $(10)_{\rm ZnO} = (0.883, 0.720)_{\rm Fe}$ and $(01)_{\rm ZnO} = (0.000, 1.440)_{\rm Fe}$, where the subscripts refer to the unit cells to which the coordinates refer.

On the basis of these coordinates we derive $a_{\rm ZnO} = 3.253 \pm 0.005$ Å very close to the value 3.2498 Å found by Abrahams *et al.* [22] for bulk ZnO at room temperature. The angle γ between the hexagonal axes is equal to 120° to within a few hundredths of a degree.

Symbols in Figs. 2(a)–2(c) represent $I_{\rm obs}(hk\ell)$ for the (10ℓ), (11ℓ), (20ℓ) and (21ℓ) rods of the 1.5 and 2.9 ML film, respectively. These rods solely originate from the ZnO film. There is no interference with the CTRs of the Fe(110) substrate crystal [23] since the ZnO film grows in an incommensurate relationship on Fe(110). Error bars correspond to the standard deviations (1σ) as outlined in Ref. [24]. We find σ to lie in the 10%–15% range.

The analysis of the atomic structure was carried out by least squares fit of $I_{\rm obs}(hk\ell)$ using the program PROMETHEUS [25]. Since all atoms occupy high symmetry positions within the plane group $p3m1$ only their z positions are free parameters. In addition one overall scale factor and one Debye parameter ($B = 8\pi^2\langle u^2\rangle$) were allowed to vary. Each data set consists of about 120 independent reflections. Solid lines in Figs. 2(a)–2(c) represent the best fits of the calculated intensities [$I_{\rm calc}(hk\ell)$] to $I_{\rm obs}(hk\ell)$. We find unweighted residuals (R_u) in the range of 20% and a goodness of fit (GOF) [26] of 0.8 and 1.0 for the 2.9 and the 1.5 ML film, respectively, which can be considered as quite satisfactory.

For both films very similar structure parameters are derived leading to oxygen terminated film surfaces. Fig. 1(d) schematically shows the model for the 2.9 ML sample. Interatomic distances are given in Å. The most important result is that

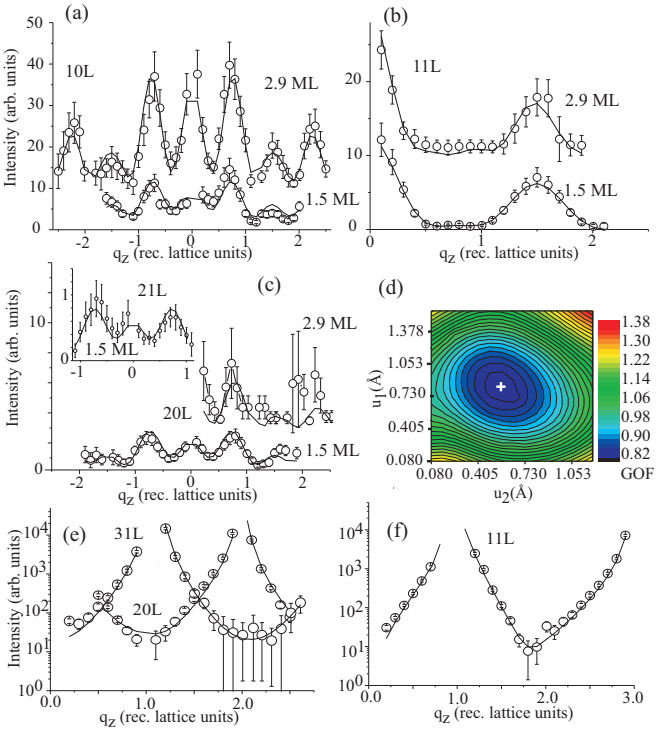

FIG. 2. (Color online) (a)-(c) Experimental (symbols) and calculated (lines) intensities along q_z for the 1.5 (lower curves) and 2.9-ML-thick (upper curves) ZnO film. Indexing of the rods corresponds to Fig. 1(b) using the relation $I(hk\ell) = I(kh\bar{\ell})$ according to the $p3m1$ symmetry. Curves are shifted for clarity. (d) Contour plot of GOF versus u_1 and u_2 for the 2.9 ML film. The white cross marks the minimum. (e) and (f) Data and fit for Fe(110) crystal truncation rods. Note the very different intensity ranges between (a)–(c) and (e) and (f).

the parameter u_j ($j = 1, \ldots, 4$), which represents the height difference between the Zn and the O atom in each double layer, lies in the range between $u_2 = 0.57$ Å (minimum) and $u_1 = 0.81$ Å (maximum). The bulk value is 0.63 Å [22]. Simultaneously, we find a vertical distance between ZnO double layers close to the bulk value of 2.6 Å in close agreement with the value of 2.5 Å derived from the STM [Fig. 1(c)].

Figure 3 summarizes the results showing in (a) the vertical distances between the Zn atoms in layers j and $j+1$ and in (b) the values u_j. Dashed lines represent respective bulk values [22]. For both films we find structure parameters which are close to those of bulk WZ, i.e., there is no indication for the presence of the h-BN structure, which in the ideal case would correspond to $u = 0.00$ Å for all layers. For comparison, for a 2.7-ML-thick ZnO film on Ag(111), Tusche *et al.* [13] found structure parameters close to the h-BN-like structure: $u_j \approx 0.2$ Å for $j = 1,2,3$ and $d_{j,j+1}$ significantly lower than 2.60 Å ($\approx$2.3 to 2.5 Å) for $j = 1,2$.

In order to estimate the accuracy of the determination of the parameters (u_j) we have carried out systematic calculations, one of which is shown in Fig. 2(d). It shows the contour plot of the GOF parameter versus u_1 and u_2. The white cross marks the minimum of GOF. Allowing for a 10%–15% increase of the GOF relative to the minimum as an estimate of the uncertainty [27], we derive uncertainties for u_j ($j = 1,2$) in the ± 0.2 Å range [see, e.g., the error bar in Fig. 3(a)].

Other structure models can be ruled out. For instance for bulk ZnO crystals sophisticated surface reconstructions which stabilize the polar $\{0001\}$ surfaces are involved, with a surface Zn:O stoichiometry different from 1:1 like $Zn_{0.75}O$ on ZnO(0001) [7,8]. First of all, the STM images of the thin film samples [see Fig. 1(c)] do not show any indication for specific surface morphologies such as triangular islands [ZnO(0001)] [8] or double layer steps [step height = 5.2 Å for ZnO(000$\bar{1}$)] which have been observed on bulk samples. In addition we have thoroughly studied the Zn:O ratio within the layers, since these defects might also play a role in surface depolarization. The SXRD analysis clearly indicates that the stoichiometry of the individual layers is close to Zn : O = 1 : 1. SXRD is well capable to derive layer stoichiometries. For instance the Zn : O = 0.75 : 1 ratio for bulk ZnO(0001) has been observed first by Jedrecy *et al.* [28]. For more details we refer to the Supplemental Material [29].

Double layer occupancies (Θ_j) which correspond to fractional occupancies of the surface, are shown in Fig. 1(a) for both samples. The uncertainties for the occupancies lie in the 10–20 percentage points regime. The observed sequence of the layer fillings correspond to imperfect layer-by-layer growth in agreement with STM. The coverage of the sample studied by STM [Fig. 1(c)] is somewhat higher than that of the 2.9 ML sample studied by SXRD. In the STM image the topmost (fourth) layer fills about 60% of the surface area and the third layer is almost complete.

In addition to the superlattice rods, also several CTRs of the Fe(110) surface were collected which are shown in Figs. 2(e) and 2(f) together with the fit (lines) with GOF ≈ 1.6 and $R_u \approx 0.15$ based on $|F|^2$ [26]. The corresponding structure model is sketched in Fig. 4 in a perspective side view. There is an almost complete occupation of the two hollow sites within the surface unit cell by oxygen [labeled by (2),(3)] which induces a considerable rumpling ($\approx$0.4 Å) within the top Fe layer [atoms (1) and (4)], but leaving the Fe-Fe interlayer bonds within 10% of the bulk (2.50 Å). The first-principles calculations confirm the oxygen-induced rumpling as due to the accommodation of oxygen in the surface and keeping the O-Fe bonds larger than 1.70 to 1.80 Å. We note that simultaneously to the SXRD experiments x-ray photoemission experiments have been carried out confirming the presence of oxygen at the ZnO/Fe(110) interface. As will be discussed in the following the presence of the interface oxygen is the key to understand why the ultrathin ZnO film adopts the WZ rather than the h-BN structure. It also explains why the films are O terminated.

Experiments were complemented with first-principles calculations using the Vienna *ab initio* simulation package (VASP) code, well known for its precise determination of energies and forces [30,31]. To model the structure within a slab geometry we used a nine-monolayer-thick substrate supercell covered on top with the ZnO films of a given thickness. A 20-Å-thick vacuum layer separates the slabs along the c axis [directions refer to the Fe(110) surface setting]. The calculations were carried out within the framework of generalized gradient approximation of the density functional theory [32].

At first, the charge density of the system with [ρ(ZnO/FeO/Fe)] and without [ρ(ZnO/Fe)] interfacial oxygen was calculated using the SXRD-derived ZnO film structure. The purpose of these simulations is to analyze the changes of the charge distribution as a result of the incorporation of the interface oxygen *without* considering structural re-

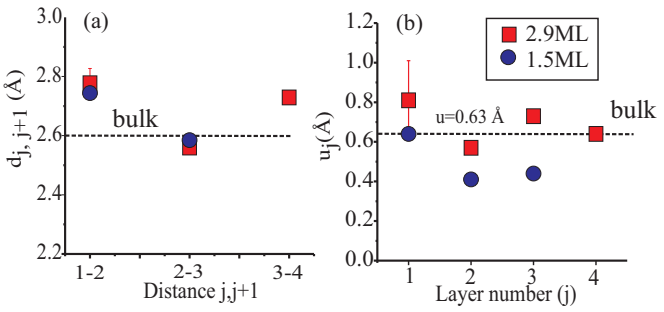

FIG. 3. (Color online) (a) Distance between Zn atoms in layers $j, j+1$. (b) Parameter u versus layer number (j) for the 1.5 and 2.9 ML samples. Corresponding values for bulk ZnO are indicated by horizontal dashed lines. Error bars are representative for all data.

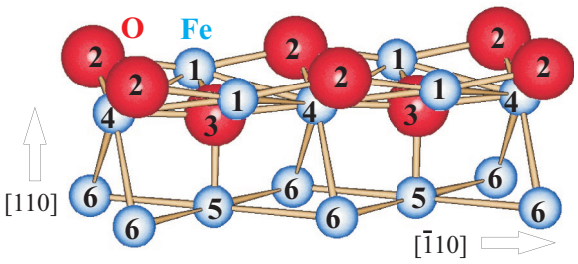

FIG. 4. (Color online) Structure model for the O/Fe(110) interface (Fe: blue; O: red). Two unit cells are shown. Atoms are labeled by (1) to (6). Some interatomic distances in Ångström units: (3)-(5): 1.78; (2)-(1): 2.05; (2)-(4): 1.70.

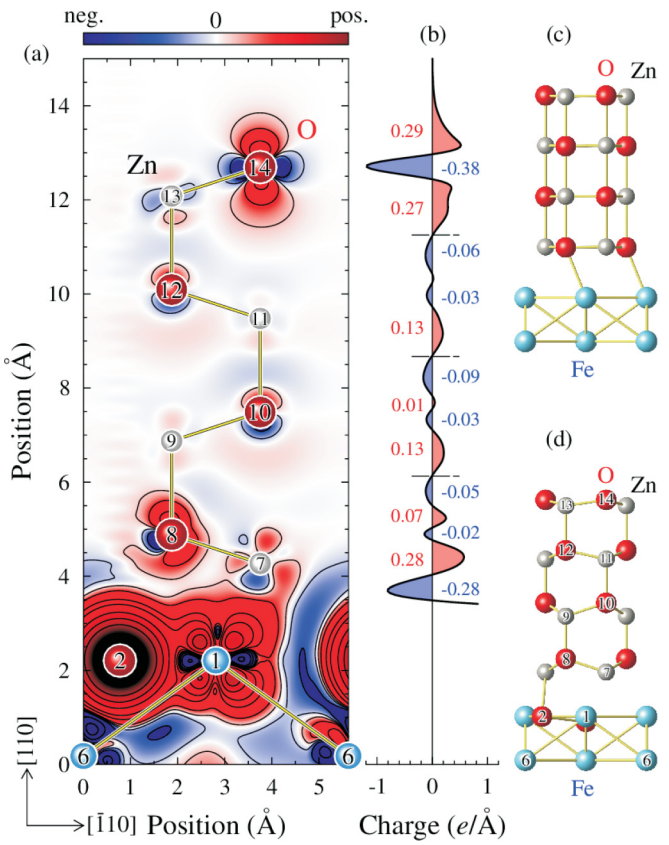

FIG. 5. (Color online) (a) Oxygen-induced charge redistribution in ZnO thin film on Fe(110), calculated as a difference of the charge densities in the geometry Fig. 3 with and without oxygen atoms (2) in the interfacial Fe layer. Red and blue colors indicate positive and negative charge density difference, respectively. Interfacial Fe and O atoms are labeled with numbers according to Fig. 4(b): Laterally integrated difference charge density ($\int_{[\bar{1}10]} \Delta\rho\, dr$). Numbers indicate difference density in electrons. Results of atomic relaxations for the cases without and with oxygen atoms in the interfacial Fe layer are shown in (c) and (d), respectively.

laxations. To facilitate the calculations the two-dimensional Fe(110) lattice was adapted to that of the ZnO film. This is because the calculation based on the experimental incommensurate relationship between film and substrate would require very large supercells making the computation unnecessarily complex, since the local charge density within the film does not strongly depend on the registry to the substrate.

The result of the calculations is presented in Fig. 5(a) which shows the difference of the charge density $\Delta\rho = \rho(\text{ZnO/FeO/Fe}) - \rho(\text{ZnO/Fe})$ in the plane through Fe atoms (1),(6) and the interfacial oxygen atom (2) (cf. Fig. 4). Red ($\Delta\rho > 0$) and blue ($\Delta\rho < 0$) difference densities correspond to electron accumulation and depletion, respectively. Figure 5(b) shows the in-plane integrated difference charge density ($\int_{[\bar{1}10]} \Delta\rho\, dr$) where the integration is carried out along the [$\bar{1}$10] direction.

The most obvious and trivial modification of the charge density distribution upon oxygen incorporation is that interfacial oxygen leads to a strong increase of charge in the plane of oxygen atom (2) and Fe atom (1) due to the strong bond between them. This reduces the bond strength between the ZnO film and the substrate, which is confirmed by the adhesion energy calculations, providing the values of 3.5 and 3.2 eV for the relaxed structure models without and with the interfacial oxygen, respectively. The reduction of the bond strength between substrate and film results in significant changes of the charge density in the vicinity of the film's surface and at the interface to the substrate: There is an increase of the ρ_z and a decrease of the $\rho_{x,y}$ charge density, respectively [atoms (8) and (14) in Fig. 5(a)]. This anisotropic charge redistribution induces a structural transformation from the h-BN structure ($u_j = 0$) to the WZ structure with ($u_j \neq 0$). Calculations allowing for structural relaxation clearly support this model: In the case of the oxygen-free interface the ZnO layers form a flat- (h-BN) type structure [see Fig. 5(c)] similar to that observed in the ZnO film on Ag(111) and Pd(111) [13,15]. By contrast, if oxygen is incorporated into the Fe(110) surface the ZnO film structure is close to the bulk WZ-type one [see Fig. 5(d)], which is in excellent agreement with experiment.

The transformation from the h-BN-type to the WZ-type structure strongly modifies the electronic structure of the surface layer. While all layers in the h-BN ZnO film are insulating, the WZ film has a metallic surface [29]. The surface metallization in thin oxide films was already reported in experimental and theoretical studies [33,34]. This electronic reconstruction is the main depolarization mechanism in the ZnO WZ film [33,35], while in the h-BN ZnO the depolarization is achieved by the atomic rearrangement [13–15].

In summary, we have presented a SXRD structure analysis of ultrathin ZnO films (1.5 and 2.9 ML) deposited on Fe(110). Evidence is given that in this coverage regime, where the h-BN structure is expected to be stable, the ZnO film adopts the bulklike WZ-type structure rather than the h-BN-type structure. This is a consequence of the anisotropic charge redistribution within the ZnO film induced by the presence of interface oxygen. Although the WZ structure is polar, its metallic surface renders its stability. Our study has provided clear evidence that in ultrathin films depolarization mechanisms involve a complex interplay between atomic and electronic structure.

The authors acknowledge support and hospitality by the staff of the ESRF and the Elettra storage ring. We thank F. Weiss for technical support. The help of O. Mironets during the experiments is also gratefully acknowledged. This work is supported by the DFG through SFB 762.

[1] M. Bäumer and H.-J. Freund, Prog. Surf. Sci. **61**, 127 (1999).
[2] M. H. Huang, S. Mao, H. Feick, H. Q. Yan, Y. Y. Wu, H. Kind, W. Weber, R. Russo, and P. D. Yang, Science **292**, 1897 (2001).
[3] G. Fischer, N. Sanchez, W. Adeagbo, M. Lüders, Z. Szotek, W. M. Temmerman, A. Ernst, W. Hergert, and M. C. Muñoz, Phys. Rev. B **84**, 205306 (2011).

[4] P. W. Tasker, J. Phys. C **12**, 4977 (1979).

[5] C. Noguera, J. Phys.: Condens. Matter **12**, R367 (2000).

[6] J. Goniakowski, F. Finocchi, and C. Noguera, Rep. Prog. Phys. **71**, 016501 (2008).

[7] O. Dulub, L. A. Boatner, and U. Diebold, Surf. Sci. **519**, 201 (2002).

[8] O. Dulub, U. Diebold, and G. Kresse, Phys. Rev. Lett. **90**, 016102 (2003).

[9] A. Calzolari, M. Bazzani, and A. Catellani, Surf. Sci. **607**, 181 (2013).

[10] W. Hebenstreit, M. Schmid, J. Redinger, R. Podloucky, and P. Varga, Phys. Rev. Lett. **85**, 5376 (2000).

[11] M. Kiguchi, S. Entani, K. Saiki, T. Goto, and A. Koma, Phys. Rev. B **68**, 115402 (2003).

[12] E. D. L. Rienks, N. Nilius, H.-P. Rust, and H.-J. Freund, Phys. Rev. B **71**, 241404 (2005).

[13] C. Tusche, H. L. Meyerheim, and J. Kirschner, Phys. Rev. Lett. **99**, 026102 (2007).

[14] H. L. Meyerheim, C. Tusche, A. Ernst, S. Ostanin, I. V. Maznichenko, K. Mohseni, N. Jedrecy, J. Zegenhagen, J. Roy, I. Mertig, and J. Kirschner, Phys. Rev. Lett. **102**, 156102 (2009).

[15] G. Weirum, G. Barcaro, A. Fortunelli, F. Weber, R. Schennach, and F. P. Netzer, J. Phys. Chem. C **114**, 15432 (2010).

[16] J. Goniakowski, C. Noguera, and L. Giordano, Phys. Rev. Lett. **98**, 205701 (2007).

[17] C. Noguera and J. Goniakowski, J. Phys.: Condens. Matter **20**, 264003 (2008).

[18] J. Goniakowski and C. Noguera, Phys. Rev. B **83**, 115413 (2011).

[19] F. Claeyessens, C. F. Freeman, N. L. Allan, Y. Sun, M. N. R. Ashfold, and J. H. Harding, J. Mater. Chem. **15**, 139 (2005).

[20] J. Kirschner, Surf. Sci. **138**, 191 (1984).

[21] We use the following setting of the Fe surface (s) cell, which is related to the bulk (b) unit cell by the relations: $[100]_s = [00\bar{1}]_b$, $[010]_s = [\bar{1}10]_b$, and $[001]_s = [110]_b$.

[22] S. C. Abrahams and J. L. Bernstein, Acta Crystallogr., Sect. B: Struct. Crystallogr. Cryst. Chem. **25**, 1233 (1969).

[23] I. K. Robinson, Phys. Rev. B **33**, 3830 (1986).

[24] I. K. Robinson, in *Handbook on Synchrotron Radiation*, edited by G. Brown and D. E. Moncton (Elsevier, New York, 1991), Vol. 3.

[25] U. H. Zucker, E. Perenthaler, W. F. Kuhs, R. Bachmann, and H. Schulz, J. Appl. Crystallogr. **16**, 358 (1983).

[26] The unweighted residual (R_u) is defined as $R_u = \sum ||I^{\rm obs}| - |I^{\rm calc}|| / \sum |I^{\rm obs}|$. GOF is defined by $\mathrm{GOF} = \sqrt{1/(N-P)\sum[(|I^{\rm obs}| - |I^{\rm calc}|)/\sigma^2]}$. Here, $I^{\rm obs}$ and $I^{\rm calc}$ are the experimental and calculated intensities, respectively, while N and P represent the number of data points and the number of refined parameters. The standard deviation of $I^{\rm obs}$ is given by σ. The summation runs over all data points.

[27] W. C. Hamilton, Acta Crystallogr. **18**, 502 (1965).

[28] N. Jedrecy, M. Sauvage-Simkin, and R. Pinchaux, Appl. Surf. Sci. **162–163**, 69 (2000).

[29] See Supplemental Material at http://link.aps.org/supplemental/10.1103/PhysRevB.90.085423 for the x-ray analysis of the Zn:O atomic ratio and for the analysis of the electronic structure of the ZnO film.

[30] G. Kresse and J. Furthmüller, Phys. Rev. B **54**, 11169 (1996).

[31] J. Hafner, J. Comput. Chem. **29**, 2044 (2008).

[32] J. P. Perdew, K. Burke, and M. Ernzerhof, Phys. Rev. Lett. **77**, 3865 (1996).

[33] R. Hesper, L. H. Tjeng, A. Heeres, and G. A. Sawatzky, Phys. Rev. B **62**, 16046 (2000).

[34] J. Goniakowski, L. Giordano, and C. Noguera, Phys. Rev. B **81**, 205404 (2010).

[35] A. Fujimori, F. Minami, and N. Tsuda, Surf. Sci. **121**, 199 (1982).